PROCEEDINGS OF SPIE

SPIEDigitalLibrary.org/conference-proceedings-of-spie

High-efficiency short-cavity III-V-on-Si C-band DFB laser diodes

J. Rahimi, J. Van Kerrebrouck, B. Haq, J. Bauwelinck, G. Roelkens, et al.

J. Rahimi, J. Van Kerrebrouck, B. Haq, J. Bauwelinck, G. Roelkens, G. Morthier, "High-efficiency short-cavity III-V-on-Si C-band DFB laser diodes," Proc. SPIE 12006, Silicon Photonics XVII, 120060H (5 March 2022); doi: 10.1117/12.2607357

SPIE.

Event: SPIE OPTO, 2022, San Francisco, California, United States

High-efficiency short-cavity III-V-on-Si C-band DFB laser diodes

J. Rahimi*[a,b] , J. Van Kerrebrouck[c], B. Haq[d], J. Bauwelinck[c], G. Roelkens[a,b], G. Morthier[a,b]
[a]Dept. of Information Technology (INTEC), Photonics Research Group, Ghent University-IMEC, 9052 Ghent, Belgium; [b]Center for Nano- and Biophotonics (NB-Photonics), Ghent University, Ghent B-9000, Belgium; [c]Dept. of Information Technology (INTEC), IDLab, Ghent University-IMEC, 9052 Ghent, Belgium; [d]GLOBALFOUNDRIES, Dresden, Germany

ABSTRACT

In this paper, we demonstrate a high-efficiency, short-cavity heterogeneously integrated C-band DFB laser on a Si waveguide realized using adhesive bonding. First, simulation results regarding the integrated cavity design are discussed. In order to decrease the optical loss inside the cavity, we designed a configuration where the optical mode inside the laser cavity is predominantly confined to the Si waveguide underneath. Then, the fabrication technology of the demonstrated device is explained. Finally, we discuss the measured static and dynamic characteristics of the integrated laser. Up to 13% wall plug efficiency is achieved for a 200 μm long DFB laser diode at 20 ºC. Up to two times 6 mW of optical power is coupled into the silicon waveguide and more than 44 dB side-mode suppression ratio is obtained. In addition, the dynamic characteristics of the device are demonstrated by non-return-to-zero on-off keying modulation at 20 Gb/s and the transmission over a 2 km long optical fiber.

Keywords: Heterogeneous integration, Direct modulation, Distributed feedback lasers, Wall-plug efficiency

1. INTRODUCTION

Heterogeneous integration of III-V materials on silicon-on-insulator (SOI) is one of the most possible approaches in realizing on chip light sources for silicon photonics (SiP) [1]. In this approach, the III-V membrane can be first bonded and then processed into active components such as lasers or it can be first processed on its own III-V substrate as coupons and then micro-transfer-printed to the pre-patterned SOI circuits [2], [3]. Since the final package size and cost of the optical transceivers play an important role for employing SiP chips in commercial applications such as datacom, high-efficiency small footprint integrated light sources are highly desirable. Among the demonstrated integrated light sources, edge emitting laser diodes such as distributed feedback (DFB) lasers or distributed Bragg reflector (DBR) lasers are the transmitter of choice when fabricating low-cost integrated transmitters for O-band and C-band wavelength division multiplexing (WDM) systems. In addition, they exhibit high modulation bandwidth and output power.
The key element in designing an integrated III-V-on-SOI cavity is to accurately analyze the optical mode profile in the III-V/Si cross-section. In order to make a short cavity, the mode has to be sufficiently confined to the active region to provide sufficient gain for lasing. On the other hand, as the optical mode is more confined in the Si waveguide underneath, it will experience lower optical absorption loss since there are no doped layers in the Si device. In addition, the impact of the sidewall scattering loss also decreases. Considering this trade-off in designing the laser cavity, there have been several demonstrations on improving the efficiency and performance of heterogeneously integrated DFB lasers in recent years. In [4], a III-V-on-silicon DFB laser based on adhesive bonding with a wall-plug efficiency of about 9% has been achieved at room temperature when including the output power of both facets. [5], [6] demonstrated high modulation speed of III-V-on-silicon lasers with large confinement factor in the III-V active region with both direct and electroabsorption modulation approaches. Low-threshold short-cavity DFB hybrid silicon lasers fabricated with a low temperature molecular bonding process have been reported in [7], [8]. Wall-plug efficiencies up to 3% and 2% were achieved at 1 mW output power for the 100 μm and 200 μm long lasers, respectively [8]. Characterization of a heterogeneously integrated DFB laser operating at O-band was demonstrated by Intel in [9]. Lasing is reported up to 150 ºC and a wall-plug efficiency of 15% is achieved at 80 ºC. However, direct modulation has not been demonstrated with these devices. In [10], [11] high performance either in terms of power consumption or modulation bandwidth has been achieved by a combination of direct bonding and epitaxial regrowth but at the expense of more complex fabrication.

Silicon Photonics XVII, edited by Graham T. Reed, Andrew P. Knights,
Proc. of SPIE Vol. 12006, 120060H · © 2022 SPIE · 0277-786X
doi: 10.1117/12.2607357

2. DESIGN AND FABRICATION

Fig. 1 shows the simplified schematic of the heterogeneously integrated DFB laser on a pre-patterned SOI circuit. The SOI platform consists of a 400 nm thick Si device layer on a 2 μm buried oxide (BOX) layer. The 200 μm long cavity is determined by a 1 μm wide, first order, quarter-wave shifted grating in the Si with a 60 nm etch depth. The 60 nm etched Si waveguide is then connected to a 180 nm etched Si waveguide in which the 180 nm etched grating couplers are incorporated. In the III-V section, the epitaxial layer stack consists of a 200 nm thick highly-doped p-InGaAs contact layer, a 1.5 μm thick p-InP cladding layer, an InGaAsP multi-quantum well (MQW) active region with 6 quantum wells surrounded by 100 nm thick separate confinement heterostructure (SCH) layers, and a n-InP contact layer with a thickness of 190 nm. The laser mesa is 2 μm wide and consists of two short spot-size converters at the ends.

The hybrid optical mode profile is shown in Fig. 2 (a). As can be seen, the optical mode is more confined to the Si waveguide. The simulated confinement factor in the MQW active region is about 4% and the effective index of the fundamental mode is 3.2480. In this structure, we designed the MQW active region to be wider than the III-V mesa in order to reduce surface recombination and decrease the effect of the sidewall scattering loss caused by the etching of the active region. In addition, in order to suppress the oscillation of higher order transverse modes in the cavity, the Bragg grating is etched only in the center of the silicon waveguide. Finally, as Fig. 2(b) depicts, the optical mode profile at the short taper tip is predominantly in the Si waveguide. This design enables the efficient coupling of the light from the III-V/Si laser into the Si waveguide circuit just by incorporating a 10 μm long taper.

The SOI circuit is fabricated by a Voyager electron beam lithography (EBL) system. First, the shallow-etched waveguide and first order grating are patterned. The cavity length determined by the 60 nm etch-depth quarter-wave shifted DFB grating section is 200 μm. In a second etch step, a 180 nm deep Si waveguide is defined by writing 5 μm trenches at the sides, together with the fiber-to-chip grating couplers. After the preparation of the SOI circuit, the III-V epitaxial layer is bonded upside-down onto the SOI waveguide wafer using an adhesive bonding. After completion of the bonding and the InP substrate removal, the laser processing starts with the deposition of a 200 nm thin SiN layer as a hard mask for the mesa definition using i-line optical lithography. The mesa is created by etching the SiN by means of a reactive ion etching (RIE) tool as well as etching of the InGaAs contact layer and InP cladding layer using inductively coupled plasma (ICP). Unlike in our previous fabrications [12], we avoid using wet etching of the InP cladding in HCl to make a V-shaped mesa. Instead, we etch down the whole InP layer with ICP which results in lower sidewall roughness compared to the case where we use HCl for etching the mesa. After this step, we again deposit SiN not only to protect the side-wall of the mesa but also to use it as a second hard mask for making a wide active region. The active region is etched using an ICP etch followed by a short selective wet etch with a H_2O:H_3PO_4:H_2O_2 solution. Afterwards, another optical lithography is carried out to deposit the Ni/Ge/Au/Ti n-contact. Subsequently, the device is passivated with SiN and BCB before depositing the Ti/Au p-contact with the same process. Finally, GSG pads with a pitch of 100 μm are created to enable the static and dynamic characterizations. More details on the fabricated device as well as the cross-section images can be found in [13].

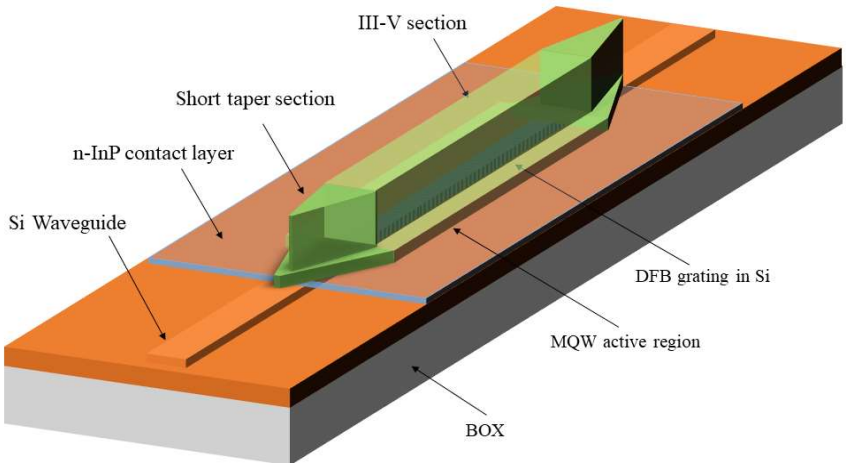

Figure 1. Schematic structure of the heterogeneously integrated DFB laser diode on the Si waveguide.

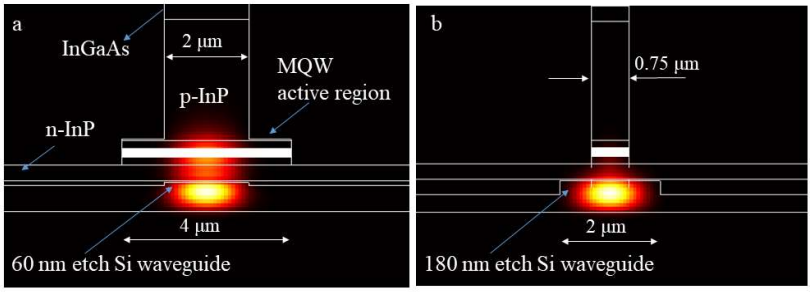

Figure 2. Optical mode profile in the III-V/Si cross-section. a) mode profile in the laser cross-section. b) mode profile at the III-V taper tip.

3. STATIC AND DYNAMIC CHARACTERISTICS

The laser's L-I curve was measured at different stage temperatures and the results are depicted in Fig. 3(a). The measured threshold current at 20 ºC is 10.5 mA and it increases up to 14.5 mA when increasing the operating temperature to 40 ºC. A waveguide-coupled optical power up to 6.5 mW is obtained from a single facet. Due to the symmetrical configuration, the same results are obtained from the other output of the laser. In addition, the measured I-V curve in Fig. 3(a) shows that the voltage remains below 2 V over operating temperatures. As it can be seen, there are ripples or kinks in the L-I curves due to the reflections from the grating coupler. The phase of these reflections changes with current due to the heating of the device. Fig. 3(b) depicts the measured optical spectrum at 20 ºC under the bias current of 70 mA. Under this bias condition, the laser operates at 1563 nm with the SMSR of about 44 dB.

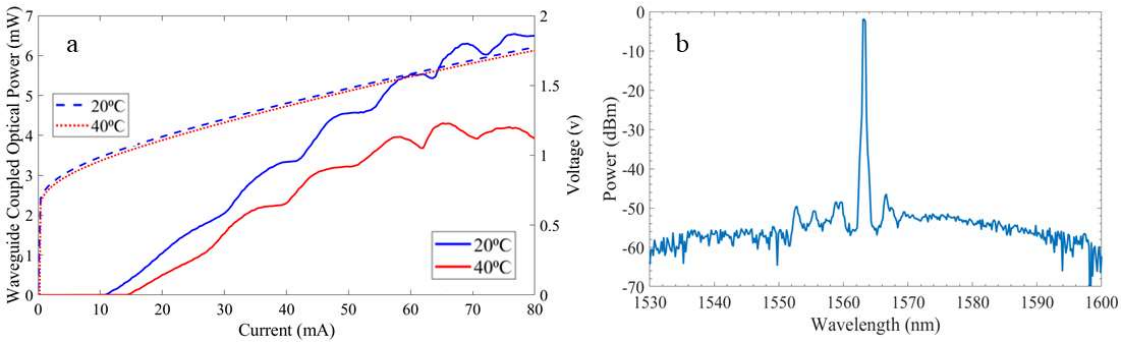

Figure 3. **(a)** Waveguide-coupled optical output power (single-sided) versus DC bias current (left), and I-V curves (right) at 20 ºC and 40 ºC. **(b)** Optical spectrum at 20 ºC at the bias current of 70 mA.

The wall-plug efficiency of the laser as a function of the bias current at different operating temperatures is shown in Fig. 4. As can be seen, up to 13% wall-plug efficiency is achievable at 20 ºC.

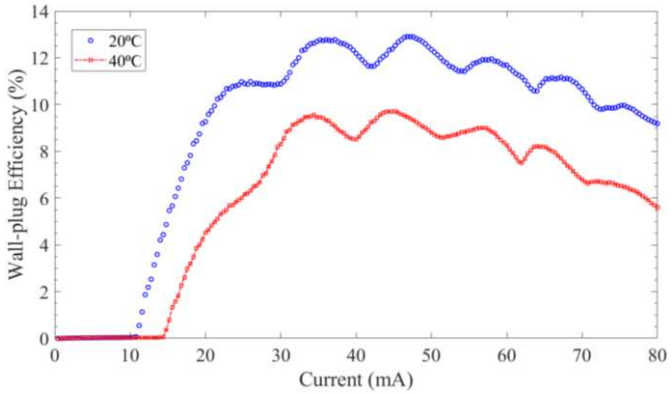

Figure 4. Wall-plug efficiency versus the bias current at 20 ºC and 40 ºC.

Small-signal measurements were carried out using an Agilent N5247A vector network analyzer (VNA) to provide radio frequency (RF) electrical signals. Using a bias tee, the RF signal is combined with a DC bias current to modulate the laser by means of a Cascade Infinity GSG RF probe with 100 μm pitch. Then, the laser light is sent to a Discovery DSC-10H photodetector (PD) with a bandwidth of 43 GHz and the output electrical signal is sent back to the VNA to measure the small signal S-parameters. Fig. 5 depicts the small signal S_{21} parameter, measured at room temperature at various bias currents. At a bias current of 60 mA the modulation bandwidth of the device is found to be around 15 GHz. The main limiting factor of the modulation bandwidth in our design (and similar ones) is the low confinement factor of the optical mode in the MQW active region. As we mentioned earlier, the optical mode in this design is mostly confined to the Si waveguide. This can be beneficial in decreasing optical loss and increasing the internal efficiency, whereas the consequence is the degradation of the modulation bandwidth.

The large signal intensity modulation of the laser is investigated by carrying out a data transmission experiment. The modulation signal is generated using a Keysight M8196A arbitrary waveform generator (AWG). An SHF807 RF amplifier is used to amplify the output signal of the AWG. Then, the amplified modulation signal is combined with a DC current via a bias tee and the corresponding output signal drives the laser by using the GSG RF probe. The laser optical output signal is directly sent to the photodetector, of which the output is fed to a Keysight 70 GHz sampling oscilloscope without using any RF amplifiers. The large signal characterization results are illustrated as eye diagrams in Fig. 6. Non-return-to-zero (NRZ) data transmission with a Pseudo-Random-Binary-Sequence (PRBS) with pattern length of 2^7-1 is verified. Open eyes can be observed at 10 Gb/s and 20 Gb/s after transmission over a 2 km long non-zero dispersion-shifted-fiber (NZ-DSF). A 4 dB extinction ratio is obtained at 20 Gb/s. These results are achieved at a bias current of 70 mA without using any optical or electrical amplifiers at the receiver, nor equalization.

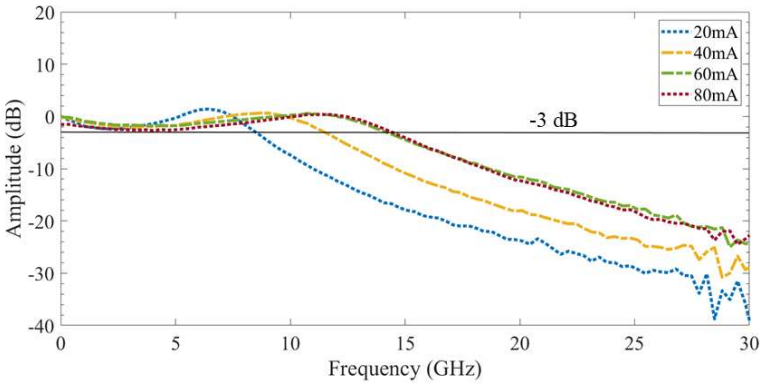

Figure 5. Small signal modulation characteristics at various bias currents.

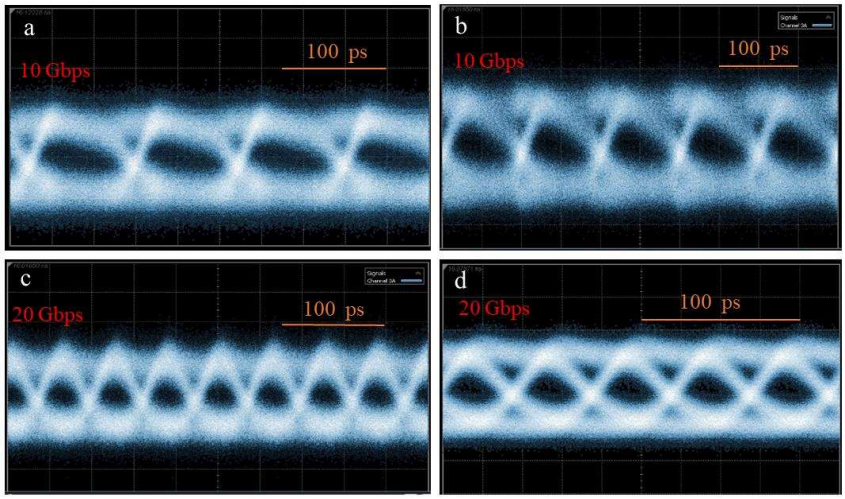

Figure 6. Data transmission experiment; (a,c) eye diagram for the back to back configuration at 10 Gb/s and 20 Gb/s, respectively. (b,d) eye diagram after transmission over a 2 km fiber at 10 Gb/s and 20 Gb/s, respectively.

4. CONCLUSION

In this work, we discuss the design, fabrication and static and dynamic characterization of high-efficiency, short-cavity DFB laser diodes, heterogeneously integrated on SOI using adhesive bonding. In order to decrease the optical loss inside the cavity, we designed a configuration where the optical mode inside the laser cavity is predominantly confined to the Si waveguide underneath. In the static characterization of the fabricated DFB laser diode, the experimental results show up to 13% wall plug efficiency at 20 ^{o}C. In addition, stable single mode operation with a SMSR larger than 44 dB is achieved. We also reported the dynamic characteristics of the laser diode by measuring the small-signal and large-signal modulation responses. Up to 15 GHz modulation bandwidth is obtained at the bias current of 60 mA. The data transmission experiment with NRZ modulation depicts open eye diagrams up to 20 Gb/s without using any equalization.

REFERENCES

[1] S. Matsuo and T. Kakitsuka, "Low-operating-energy directly modulated lasers for short-distance optical interconnects," *Adv. Opt. Photonics*, vol. 10, no. 3, p. 567, 2018, doi: 10.1364/aop.10.000567.

[2] A. W. Fang, H. Park, O. Cohen, R. Jones, M. J. Paniccia, and J. E. Bowers, "Electrically pumped hybrid AlGaInAs-silicon evanescent laser," *Opt. Express*, vol. 14, no. 20, p. 9203, 2006, doi: 10.1364/oe.14.009203.

[3] J. Zhang *et al.*, "III-V-on-Si photonic integrated circuits realized using micro-transfer-printing," *APL Photonics*, vol. 4, no. 11, 2019, doi: 10.1063/1.5120004.

[4] S. Keyvaninia *et al.*, "Heterogeneously integrated III-V/silicon distributed feedback lasers," *Opt. Lett.*, vol. 38, no. 24, p. 5434, 2013, doi: 10.1364/ol.38.005434.

[5] A. Abbasi *et al.*, "Direct and Electroabsorption Modulation of a III-V-on-Silicon DFB Laser at 56 Gb/s," *IEEE J. Sel. Top. Quantum Electron.*, vol. 23, no. 6, 2017, doi: 10.1109/JSTQE.2017.2708606.

[6] M. Shahin *et al.*, "80-Gbps NRZ-OOK Electro-Absorption Modulation of InP-on-Si DFB Laser Diodes," *IEEE Photonics Technol. Lett.*, vol. 31, no. 7, pp. 533–536, 2019, doi: 10.1109/LPT.2019.2900518.

[7] C. Zhang, S. Zhang, J. D. Peters, and J. E. Bowers, "8 × 8 × 40 Gbps fully integrated silicon photonic network on chip," *Optica*, vol. 3, no. 7, p. 785, 2016, doi: 10.1364/optica.3.000785.

[8] C. Zhang, S. Srinivasan, Y. Tang, M. J. R. Heck, M. L. Davenport, and J. E. Bowers, "Low threshold and high speed short cavity distributed feedback hybrid silicon lasers," *Opt. Express*, vol. 22, no. 9, p. 10202, 2014, doi: 10.1364/oe.22.010202.

[9] R. Jones *et al.*, "Heterogeneously Integrated InP/Silicon Photonics: Fabricating fully functional transceivers," *IEEE Nanotechnol. Mag.*, vol. 13, no. 2, pp. 17–26, 2019, doi: 10.1109/MNANO.2019.2891369.

[10] S. Yamaoka *et al.*, "Directly modulated membrane lasers with 108 GHz bandwidth on a high-thermal-conductivity silicon carbide substrate," *Nat. Photonics*, vol. 15, no. 1, pp. 28–35, 2021, doi: 10.1038/s41566-020-00700-y.

[11] N. P. Diamantopoulos *et al.*, "47.5 Ghz Membrane-Iii-V-on-Si Directly Modulated Laser for Sub-Pj/Bit 100-Gbps Transmission," *Photonics*, vol. 8, no. 2, pp. 1–11, 2021, doi: 10.3390/photonics8020031.

[12] B. Haq et al., "Micro-transfer-printed III-V-on-silicon C-band distributed feedback lasers," Opt. Exp., vol. 28, no. 22, pp. 32793–32801, 2020.

[13] J. Rahimi, J. Van Kerrebrouck, J. Bauwelinck, B. Haq, G. Roelkens, and G. Morthier, "Demonstration of a high-efficiency short-cavity III-V-on-Si C-band DFB laser diode," *IEEE J. Sel. Top. Quantum Electron.*, vol. 28, no. 3, 2022, doi: 10.1109/JSTQE.2021.3122552.